ChemPubSoc Europe

DOI: 10.1002/chem.201404967

CHEMISTRY
A European Journal
Full Paper

Dynamic Nuclear Polarization |*Hot Paper*|

Long-Lived States of Magnetically Equivalent Spins Populated by Dissolution-DNP and Revealed by Enzymatic Reactions**

Aurélien Bornet,*[a] Xiao Ji,[a] Daniele Mammoli,[a] Basile Vuichoud,[a] Jonas Milani,[a] Geoffrey Bodenhausen,*[a, b, c, d] and Sami Jannin[a, e]

Abstract: Hyperpolarization by dissolution dynamic nuclear polarization (D-DNP) offers a way of enhancing NMR signals by up to five orders of magnitude in metabolites and other small molecules. Nevertheless, the lifetime of hyperpolarization is inexorably limited, as it decays toward thermal equilibrium with the nuclear spin-lattice relaxation time. This lifetime can be extended by storing the hyperpolarization in the form of long-lived states (LLS) that are immune to most dominant relaxation mechanisms. Levitt and co-workers have shown how LLS can be prepared for a pair of inequivalent spins by D-DNP. Here, we demonstrate that this approach can also be applied to magnetically equivalent pairs of spins such as the two protons of fumarate, which can have very long LLS lifetimes. As in the case of *para*-hydrogen, these hyperpolarized equivalent LLS (HELLS) are not magnetically active. However, a chemical reaction such as the enzymatic conversion of fumarate into malate can break the magnetic equivalence and reveal intense NMR signals.

Introduction

Spin hyperpolarization by dissolution dynamic nuclear polarization (D-DNP) has become a major area of research in NMR. This emerging method provides a way of boosting the sensitivity of NMR experiments by enhancing the intrinsically low nuclear spin polarization dictated by Boltzmann's law. Thus, ^{13}C NMR signals of small molecules have been enhanced by up to four orders of magnitude.[1] In a typical D-DNP experiment, the frozen sample is initially polarized at low temperatures and moderate fields, and the signals are subsequently measured in solution in a separate detection apparatus operating at room temperature. This implies that the polarized frozen sample needs to be dissolved and transferred rapidly. This transfer, sometimes poetically called *voyage*, can be performed either manually or by means of a pneumatic system. During the voyage, the hyperpolarized molecules experience low magnetic fields (sometimes as low as the earth's field, or even lower), which have detrimental effects on the enhanced polarization. This is one of the reasons why D-DNP has been most useful for nuclear spins with long T_1, such as the isolated low-gamma quaternary ^{13}C spin in 1-^{13}C pyruvic acid.[2] On the other hand, apart from some exotic experiments,[3] ^1H spins have hardly been exploited by D-DNP, as their short T_1 relaxation times mean that the hyperpolarization is driven back rapidly toward Boltzmann equilibrium. However, we have shown recently that ^1H can be polarized very efficiently and rapidly up to $P_Z(^1H) = 91\%$ with a buildup time constant as short as $\tau_{DNP}(^1H) = 150$ s at $B_0 = 6.7$ T and $T = 1.2$ K.[4] One possible strategy for taking advantage of this large ^1H hyperpolarization consists in storing the magnetization in the form of long-lived states (LLS)[5] with extended lifetimes.

In recent years, several successful studies combining D-DNP with LLS[6] have shown that hyperpolarized magnetization can be converted into LLS with extended lifetimes $T_{LLS} \gg T_1$. In a pair of equivalent spins $^1/_2$, the singlet state $S_0 = (|\alpha\beta\rangle - |\beta\alpha\rangle)/\sqrt{2}$ is largely disconnected from the triplet states $T_{+1} = |\alpha\alpha\rangle$, $T_0 = (|\alpha\beta\rangle + |\beta\alpha\rangle)/\sqrt{2}$ and $T_{-1} = |\beta\beta\rangle$ because relaxation mechanisms that are symmetric with respect to spin exchange (such as the dipole–dipole interaction between the two spins) cannot induce singlet–triplet transitions.[7] Therefore, if a triplet–singlet population imbalance (TSI) is prepared by any means, it is likely to be long-lived. We use the expression TSI in analogy to the A/E imbalance (AEI) recently described for

[a] *A. Bornet, X. Ji, D. Mammoli, B. Vuichoud, J. Milani, Prof. G. Bodenhausen, Dr. S. Jannin*
Institut des Sciences et Ingénierie Chimiques
Ecole Polytechnique Fédérale de Lausanne
1015 Lausanne (Switzerland)
Fax: (+41) 76-693-9435
E-mail: aurelien.bornet@epfl.ch
geoffrey.bodenhausen@epfl.ch

[b] *Prof. G. Bodenhausen*
École Normale Supérieure-PSL Research University
Département de Chimie, 24 rue Lhomond, 75005 Paris (France)

[c] *Prof. G. Bodenhausen*
Sorbonne Universités
UPMC Univ Paris 06, 4 place Jussieu, 75005 Paris (France)

[d] *Prof. G. Bodenhausen*
CNRS, UMR 7203 LBM, 75005 Paris (France)

[e] *Dr. S. Jannin*
Bruker BioSpin AG
Industriestrasse 26, 8117 Fällanden (Switzerland)

[**] *DNP = Dynamic nuclear polarization*

methyl groups by Benno Meier et al.[8] Both TSI and AEI refer to a difference between the average populations of spin states belonging to different irreducible representations of the spin permutation group, that is, Γ_A and Γ_E in methyl groups and Γ_g and Γ_u (or triplet and singlet states) in pairs of equivalent spins. The excitation and detection of an LLS involving a pair of equivalent spins is challenging because the magnetic equivalence needs to be lifted during both excitation and detection but preserved during storage. In this context, two possible scenarios are: 1) in most experiments described so far, the symmetry is imposed on an otherwise inequivalent two-spin system during the storage period only, or 2) in this work, the symmetry of an inherently equivalent two-spin system is broken during both excitation and detection.

Para-hydrogen[9] offers the best example of nuclear singlet order in a molecule with two equivalent spins. The singlet state of H_2 can be produced at low temperatures (typically 40 K) in the presence of a paramagnetic catalyst, which allows singlet–triplet interconversion by lifting the symmetry of H_2 near the catalytic surface. The singlet spin state of H_2 has the lowest energy, primarily determined by the quantization of its rotational state, and therefore, is predominantly populated at low temperatures. This leads to the creation of a large TSI compared to H_2 in Boltzmann equilibrium at room temperature. *Para*-H_2 is not magnetically active, and therefore cannot be observed directly by NMR, but it can be converted into observable signals through an asymmetric hydrogenation reaction by which the two protons stemming from *para*-H_2 become inequivalent. On the other hand, a symmetric hydrogenation process can generate a molecule in which the equivalence of the two protons is preserved. This is the case, for example, for the hydrogenation of acetylene to form ethylene,[10] or of dimethyl acetylene dicarboxylate to produce dimethyl maleate.[11] The preserved *para* state can subsequently be rendered accessible to NMR by another chemical reaction that lifts the symmetry of the molecule.

If one starts with an inequivalent two-spin system, a precursor state, that is, a state that acquires a long-lived property as soon as the two spins are made equivalent during the storage interval, can be prepared by using suitable *rf* pulse sequences,[12] by adiabatic transport to low fields,[13] or by chemical reactions.[6b] Alternatively, a compromise can be found by using systems containing nearly equivalent spins[14] in which the singlet and triplet states are only weakly mixed, but with an admixture that can be augmented by suitable pulse sequences to induce a singlet-to-magnetization (S2M) conversion.

Most experiments in which D-DNP is combined with LLS[6a–e] rely on *rf* pulse sequences to prepare the LLS, usually *after* the transfer of the hyperpolarized sample to the detection magnet. As a result, extensive relaxation occurs during the transfer. However, Tayler and co-workers[6f] have shown that LLS order can be populated directly before the transfer by D-DNP for the two inequivalent ^{13}C spins in 1,2-$^{13}C_2$-pyruvic acid. They pointed out that the polarization of the singlet state P_s ($=P_{TSI}$, vide supra) is proportional to the square of the spin Zeeman polarization P_Z (i.e., $P_{TSI}=P_s=-{}^1/_3P_Z{}^2$). Therefore, provided a high spin polarization can be reached by D-DNP, say $P_Z=50\,\%$, a significant amount of singlet order, in this example $P_{TSI}=8.33\,\%$, can be created directly without any *rf* pulses. In the case where $P_Z=91\,\%$ can be attained, one obtains $P_{TSI}=28\,\%$. Such high levels of polarization can indeed be prepared directly by DNP for ^1H at $B_0=6.7$ T and $T=1.2$ K and indirectly for ^{13}C or other nuclei through cross polarization from protons.[4]

In this work, we demonstrate that a TSI can be efficiently populated by D-DNP for the pair of magnetically equivalent ^1H spins in fumarate, and that this is preserved in the liquid state after dissolution for a long time T_{TSI}, which was estimated to be of the order of 50 s. We refer to this type of LLS as hyperpolarized equivalent long-lived states (HELLS). We show how HELLS can be readily "revealed" by allowing fumarate to undergo a biologically relevant enzymatic conversion into malate.

Experiments

For efficient D-DNP, the samples usually consist of frozen glassy solids containing typically 10–50 mM polarizing agents such as TEMPOL in addition to the molecules of interest. In our experiment, the molecule of interest shall possess two spins *I* and *S* that are magnetically equivalent in the liquid phase, but inequivalent in the frozen state and in moderate magnetic fields because they are exposed to slightly different environments and therefore experience different chemical shifts because of chemical shift anisotropies (CSAs) and different internuclear and electron–nuclear dipolar couplings. Given that freezing to low temperatures lifts the equivalence, the energy levels are better expressed in the product basis (PB). At $T=1.2$ K and $B_0=6.7$ T, the proton Boltzmann polarization without DNP is $P_Z=0.57\,\%$. Therefore, the deviations of diagonal elements from the demagnetized state $\Delta\sigma=\sigma-E$ will be $(\Delta n_{\alpha\alpha}, \Delta n_{\alpha\beta}, \Delta n_{\beta\alpha}, \Delta n_{\beta\beta})={}^1/_4(2P_Z+P_Z{}^2, -P_Z{}^2, -P_Z{}^2, -2P_Z+P_Z{}^2)=(0.003, 0, 0, -0.003)$. Assuming, for simplicity, that DNP could confer a Zeeman polarization $P_Z=100\,\%$, only the lowest energy level $|\alpha\alpha\rangle$ would be populated by hyperpolarization, so that $(\Delta n_{\alpha\alpha}, \Delta n_{\alpha\beta}, \Delta n_{\beta\alpha}, \Delta n_{\beta\beta})=(0.75, -0.25, -0.25, -0.25)$ (See Figure 1a: TSI Preparation). As soon as the polarized sample is heated and dissolved to the liquid state, CSAs and dipolar couplings are averaged out, so that the spins *I* and *S* become magnetically equivalent. The density operator can therefore better be expressed in the singlet–triplet basis (STB). In our case, as $n_{\alpha\beta}=n_{\beta\alpha}$, (and hence $\Delta n_{\alpha\beta}=\Delta n_{\beta\alpha}$), it is easily seen that $\sigma(PB)=\sigma(STB)$ [and hence $\Delta\sigma(PB)=\Delta\sigma(STB)$], with the following diagonal elements: $(\Delta n_{\alpha\alpha}, \Delta n_{\alpha\beta}, \Delta n_{\beta\alpha}, \Delta n_{\beta\beta})=(\Delta n_{T+1}, \Delta n_{T0}, \Delta n_{S0}, \Delta n_{T-1})={}^1/_4(2P_Z+P_Z{}^2, -P_Z{}^2, -P_Z{}^2, -2P_Z+P_Z{}^2)$. Hence, $P_{TSI}=\Delta n_{S0}-{}^1/_3(\Delta n_{T+1}+\Delta n_{T0}+\Delta n_{T-1})=-P_z{}^2/3$. The TSI will thus result from the depletion of $n_{\alpha\beta}$ and $n_{\beta\alpha}$ by hyperpolarization (Figure 1b). The spins are equivalent, so the TSI can be stored indifferently in a low or high magnetic field (in a magnetic path for example). During the storage period, the populations of the three triplet states will equilibrate, that is, the deviations of the population of the three triplet levels will average out to give $(\Delta n_{T+1})'=(\Delta n_{T0})'=(\Delta n_{T-1})'={}^1/_3(\Delta n_{T+1}+\Delta n_{T0}+\Delta n_{T-1})={}^1/_4P_Z{}^2/3$. The singlet should not be affected by dipole–dipole relaxation, so the TSI in principle remains equal to $P_{TSI}=-P_Z{}^2/3$.

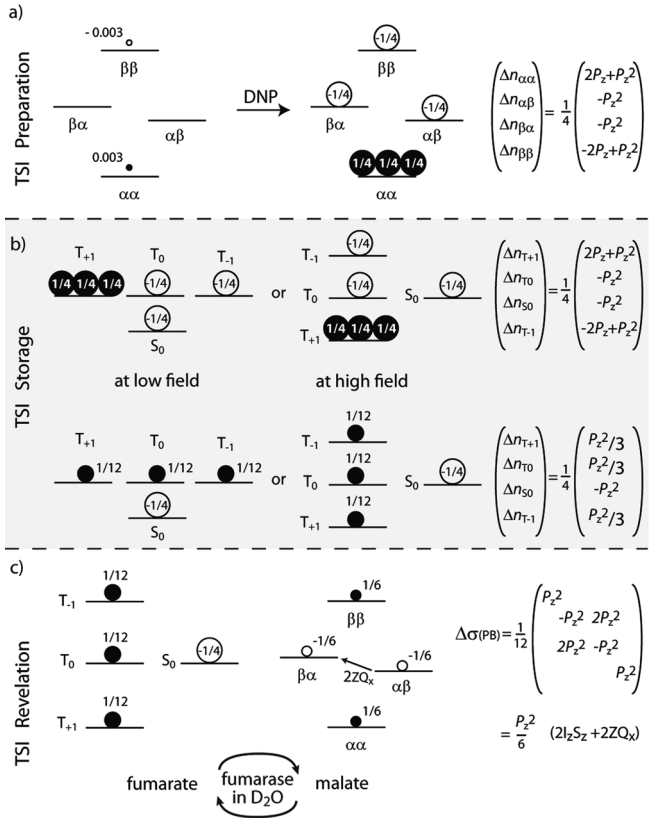

Figure 1. Schematic deviations of the populations from the fully saturated state $\Delta\sigma = \sigma - E$ among the energy levels of the two protons of fumarate a) in the polarizer at 6.7 T and 1.2 K without DNP at Boltzmann equilibrium ($P_Z(^1H) = 0.57\,\%$) and after DNP polarization to the theoretical limit $P_Z(^1H) = 100\,\%$, b) during the transfer, which may go through low magnetic fields or through a magnetic tunnel to sustain a higher field, and c) in the detection magnet, typically at 7 T and 300 K, where the spins are made inequivalent by an enzymatic conversion. In each scheme, the deviations of the diagonal elements from the demagnetized state $\Delta\sigma = \sigma - E$ are given as a function of the polarization P_z. In (c), the full density matrix is given to show the off-diagonal elements.

(See Figure 1 b: TSI storage). The sample is then transferred to the NMR or MRI magnet for detection. The system of two equivalent spins can then be transformed (chemically or enzymatically) into a system of two *in*equivalent spins, so that the "sealed" hyperpolarization can be "revealed" by conversion into observable magnetization. If the reaction is fast and goes to completion, one can convert $\Delta\sigma$ from the STB back to the PB by using a suitable base transformation (see Ref. [15]). $\Delta\sigma$(PB) resulting from this transformation can be expressed as a superposition of longitudinal two-spin order and zero-quantum coherence since $\Delta\sigma(\mathrm{PB}) = P_z^2/6\,(2I_zS_z + 2ZQ_x)$. (See Figure 1 c: TSI revelation).

Enzymatic reactions are not instantaneous, and do not necessarily lead to complete conversion into the product. Figure 2 shows an example of the conversion of fumarate into malate by fumarase under conditions that can be combined with D-DNP. The steady-state concentrations are only reached after 25 min. This has important implications for our experiment. In fact, a highly polarized state $\Delta\sigma = 2I_zS_z + 2ZQ_x$ is indeed produced instantaneously in malate whenever fumarate molecules

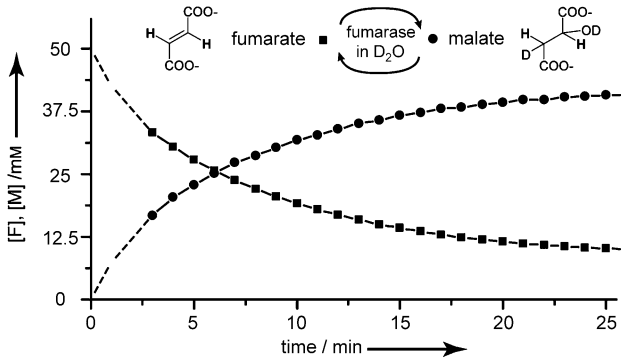

Figure 2. Enzymatic conversion of fumarate into malate by fumarase at 300 K monitored by integration of the conventional ^{1}H NMR signals of the two species. The nuclear polarizations are in thermal Boltzmann equilibrium, without resorting to DNP. A solution of fumarase (4 μL, 5.8 mg mL^{-1}, i.e., 10 units) was injected into a fumarate solution (500 μL, 50 mM) at pH 8 in a buffer of 25 mM TRIS and 200 mM NaCl.

carrying a TSI undergo an enzymatic conversion, but the ZQ_x term immediately starts evolving under the difference of chemical shifts, and therefore rapidly dephases and averages to zero as the reaction proceeds. Furthermore, the hyperpolarized TSI of fumarate, once it is transferred to malate, will tend to relax to thermal Boltzmann equilibrium.

It is, however, possible to "sustain" the LLS of malate by so-called "high-field" methods,[7c, 12, 15b] for example, by applying an *rf* irradiation halfway between the two chemical shifts (either continuous-wave (CW), or, if desired, by applying a WALTZ-16 pulse train),[16] thus preserving the full $\Delta\sigma = 2I_zS_z + 2ZQ_x$ state. This strategy allows one to slow down relaxation of $2I_zS_z$ and prevent dephasing of ZQ_x. For the two inequivalent protons in malate, we thus determined $T_{LLS} = 6$ s at $B_0 = 7$ T and $T = 298$ K. Moreover, the use of WALTZ-16 pulse trains has the advantage of wiping out any single-quantum magnetization that would not arise from HELLS. A conventional LLS detection sequence, for example, the second half of the "Sarkar sequence"[15b](Fig-

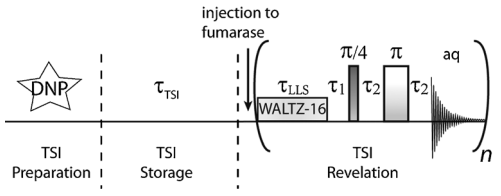

Figure 3. Timing of a HELLS experiment. After dissolution, the hyperpolarized solution containing fumarate that carries the TSI is transferred to a holding chamber just above the NMR tube to determine its lifetime T_{TSI} during a variable preinjection delay τ_{TSI}. The fumarate solution is then injected into a solution containing fumarase to start the conversion of fumarate into malate, accompanied by a conversion of the TSI on fumarate into an LLS on malate. A WALTZ-16 pulse train is applied during the delay τ_{LLS} with the carrier halfway between the chemical shifts of the two protons of malate to make these two protons effectively equivalent. The remainder of the pulse sequence is identical to the second half of the "Sarkar sequence".[15b] The conversion of the LLS into observable magnetization is most efficient when $\tau_1 = 1/(4\,J_{IS})$and $\tau_2 = 1/(2\Delta\nu_{IS})$($J_{IS} = 10.4$ Hz and $\Delta\nu_{IS} = 960$ Hz at 300 MHz). The detection scheme can be repeated n times, bearing in mind that the LLS on malate is replenished during each sustaining interval τ_{LLS} by enzymatic conversion of fumarate that carries a slowly relaxing TSI.

ure 3), can then be used to transform $\Delta\sigma = 2I_zS_z + 2ZQ_x$ into observable magnetization.

The lifetime of the LLS of malate ($T_{LLS}^{M} = 6$ s at 300 MHz if the *rf* amplitude of the CW field is $\nu_1 = 3$ kHz) is short compared to the enzymatic transformation, so the time τ_{LLS} (see Figure 3) allocated for the LLS to accumulate in malate before it is converted into observable signals needs to be optimized carefully. The concentrations [*F*] and [*M*] of fumarate and malate can be described by pseudo first-order kinetics as shown in Equation (1), in which [*F*](t) and [*M*](t) are the concentrations of fumarate and malate, k_{FM} and k_{MF} are the apparent kinetic constants of the overall enzymatic conversion of fumarate into malate and vice versa, without considering the details of the Michaelis–Menten mechanism.

$$\begin{cases} \frac{d[F](t)}{dt} = -k_{FM}[F](t) + k_{MF}[M](t) \\ \frac{d[M](t)}{dt} = -k_{MF}[M](t) + k_{FM}[F](t) \end{cases} \quad (1)$$

The temporal evolution of the expectation value P_{LLS}^{M} in malate arising from the conversion of fumarate can be obtained by solving numerically the rate equations [Eq. (2)], in which P_{TSI}^{F} and P_{LLS}^{M} are the expectation values of the TSI in fumarate and of the LLS in malate, and R_{TSI}^{F} and R_{LLS}^{M} are their relaxation rates.

$$\begin{cases} \frac{dP_{TSI}^{F}(t)}{dt} = -\left(k_{FM} + R_{TSI}^{F}\right)P_{TSI}^{F}(t) + k_{MF}P_{LLS}^{M}(T) \\ \frac{dP_{LLS}^{M}(t)}{dt} = -\left(k_{MF} + R_{LLS}^{M}\right)P_{LLS}^{M}(t) + k_{FM}P_{TSI}^{F}(T) \end{cases} \quad (2)$$

The "apparent" rate constants k_{FM} and k_{MF} can be obtained by fitting the signal amplitudes in Figure 2 to the rate equations in Equation (1). One can then calculate the temporal evolution of P_{TSI}^{F} in fumarate in the presence of ten units of enzyme, as well as P_{LLS}^{M} of malate obtained by the conversion of the TSI of fumarate into an LLS of malate that relaxes with T_{LLS}^{M} (Figure 4). These curves were obtained by assuming that $T_{TSI}^{F} = 60$ s for fumarate (on the basis of preliminary observations as discussed below), and using the experimentally determined time constant $T_{LLS}^{M} = 6$ s for malate. According to Figure 4, the optimal delay to maximize the conversion of the TSI of fumarate into the LLS of malate is 10 s. Thus, one should wait $\tau_{LLS} = 10$ s while sustaining the LLS by a suitable *rf* field before attempting to convert the LLS of malate into observable magnetization. The alternation of *rf* irradiation and signal observation can be repeated *n* times. During each interval τ_{LLS}, the LLS on malate will be replenished by the enzymatic conversion of the slowly relaxing TSI of fumarate. The decay of the magnetically silent TSI of fumarate will be reflected indirectly in the decay of the malate signal as *n* increases. Moreover, it can be seen in Figure 4b that only around 1% of the HELLS of fumarate is transferred to malate during each loop $n = 1, 2, \ldots, N$.

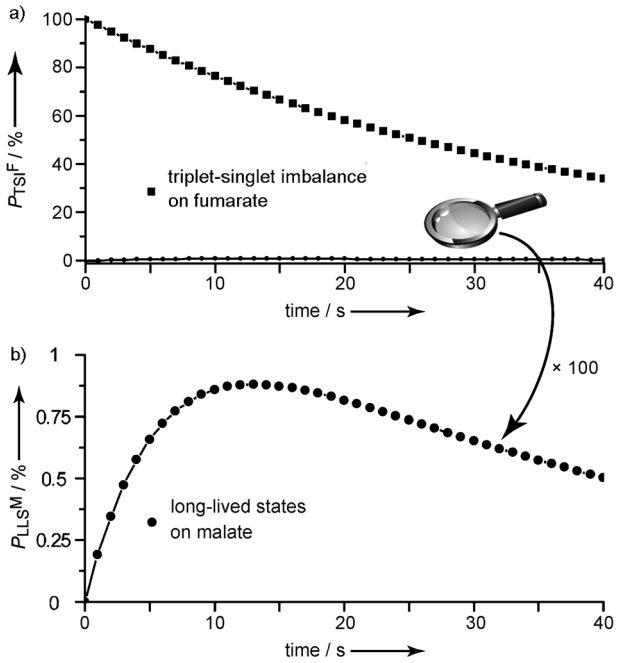

Figure 4. a) Temporal evolution of the (unobservable) P_{TSI} of fumarate and b) signal of malate obtained by numerical solution of Equation (2) with $T_{TSI}^{F} = 60$ s and $T_{LLS}^{M} = 6$ s, and the apparent forward and backward rate constants $k_{MF} = 4.5 \times 10^{-4}$ s^{-1} and $k_{FM} = 3.7 \times 10^{-4}$ s$^{-1} = 0.825\ k_{MF}$ optimized by fitting the curves in Figure 2. The vertical scale was increased 100 times in (b) to show the malate signal, which is barely visible as (-●-) in (a) because of the slow rate of the enzymatic conversion.

Results

A sample comprising ten frozen pellets of 10 μL each of 0.5 M fumarate with 50 mM TEMPOL was hyperpolarized by microwave irradiation at $B_0 = 6.7$ T and $T = 1.2$ K for about 20 min. The sample was then dissolved, together with ten frozen pellets of 10 μL each of 3 M sodium ascorbate in D_2O,[17] with 5 mL D_2O at 400 K and 1.0 MPa, and transferred in 4.5 s to a holding chamber just above the magnetic center of a 7 T NMR (300 MHz) spectrometer, where the static field is $B_{hold} > 6.5$ T. After a preinjection delay $1 < \tau_{TSI} < 60$ s, which allows one to assess the lifetime T_{TSI} of the TSI (P_{TSI}) of hyperpolarized fumarate in the holding chamber, the solution was injected into a 5 mm NMR tube containing fumarase to start the conversion of fumarate into malate, and to transfer concomitantly the TSI of fumarate into an LLS on malate. The latter was sustained by a WALTZ-16 pulse train with an *rf* amplitude $\nu_1 = 3$ kHz. The sequence of Figure 3 was then used to convert the LLS of malate into observable magnetization.

Figure 5d shows four spectra of malate acquired at 7 s intervals ($N = 4$ loops, each comprising a sustaining interval $\tau_{LLS} = 6$ s and an acquisition time of 1 s) after the injection of hyperpolarized fumarate into the NMR tube containing fumarase. In this case, the preinjection delay $\tau_{TSI} = 1$ s during which the fumarate was kept in the holding chamber was negligible compared with T_{TSI}^{F}. The enzymatic conversion is relatively slow, so the signals in Figure 5d arise from the conversion of a small fraction of fumarate into malate (≈1% every 7 s, according to

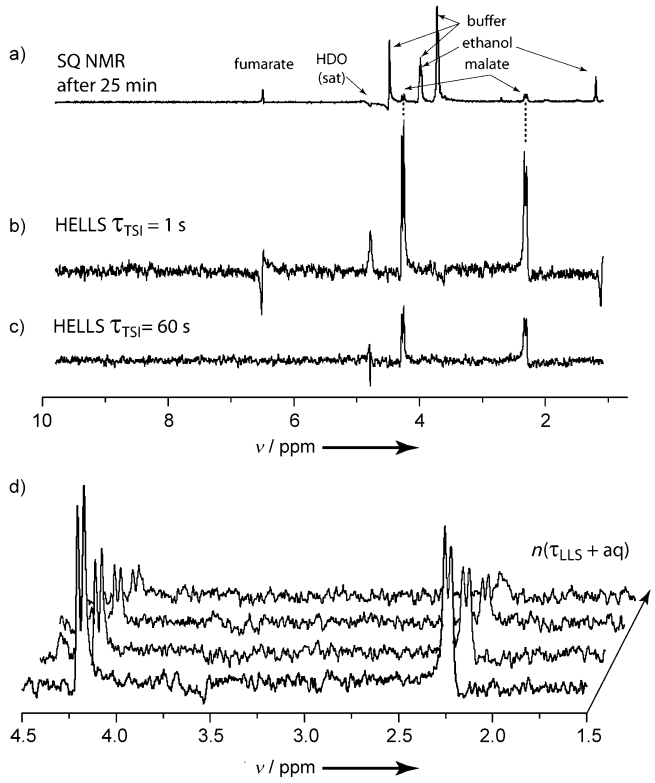

Figure 5. a) Conventional NMR spectrum excited by a 90° pulse 25 min after injection into a solution containing fumarase, when the enzymatic reaction has reached a steady state and the hyperpolarization (both P_{TSI}^{F} in fumarate and P_{LLS}^{M} in malate) has decayed to thermal equilibrium. Note the signals of fumarate, malate, ethanol, and buffer. The HDO peak was attenuated by presaturation with a selective pulse with an *rf* amplitude of 75 Hz and a duration of 5 s. b) Spectrum of malate (without significant stopover in the holding chamber since $\tau_{TSI} = 1\ s \ll T_{TSI}^{F}$) recorded with the sequence of Figure 3, shortly after injection ($n = 1$) into a solution containing fumarase in the 7 T NMR system. c) Spectrum of malate recorded after keeping the hyperpolarized fumarate for $\tau_{TSI} = 60$ s in the holding chamber at $B_0 > 6.5$ T prior to injection into the fumarase solution. d) The first four spectra of malate acquired with $n = 1$, 2, 3, and 4 at intervals of 7 s using the sequence in Figure 3 ($\tau_{TSI} = 1$ s, $\tau_{LLS} = 6$ s, acquisition time 1 s) showing that P_{LLS}^{M} is replenished through the enzymatic reaction.

Figure 4b). The decay of the malate signal with increasing n reflects 1) the decay of the inaccessible TSI of fumarate with a time constant T_{TSI}^{F} owing to its relaxation (believed to be very slow), 2) the consumption of fumarate with a time constant $1/k_{FM}$ owing to its enzymatic conversion into malate, and 3) the decay of the LLS of malate with a time constant $T_{LLS}^{M} =$ 6 s (Figure 4a). However, it is risky to extract a reliable estimate of T_{TSI}^{F} from numerical fits of a single decay.

The lifetime T_{TSI}^{F} can be estimated more accurately by repeating the entire experiment such that the fumarate that carries the hyperpolarized TSI is kept in the holding chamber during a longer preinjection delay $\tau_{TSI} = 60$ s. Although it is challenging to reproduce the experiment under identical conditions, we observed that the remaining signal of malate after $\tau_{TSI} = 60$ s was reduced by a factor of approximately 3.5 (Figure 5b,c), implying that $T_{TSI}^{F} \approx 50$ s. This is somewhat shorter than the lifetime $T_{TSI} = 270$ s reported by Zhang et al.[11] for deuterated dimethyl maleate produced by the addition of *para*-H_2 to deuterated dimethyl acetylene dicarboxylate. This discrepancy may be caused by the presence of dissolved paramagnetic triplet oxygen in the superheated water used in our dissolution experiments, or to the presence of some residual TEMPOL radicals, as the reduction by ascorbate may not be quantitative. Because the WALTZ-16 pulse train destroys magnetization arising from any sources other than HELLS, single-quantum terms arising either from D-DNP or from a partial return to thermal Boltzmann equilibrium are wiped out (compare Figure 5b,c with Figure 5a). The detected signals can therefore unambiguously be traced back to the TSI of fumarate prepared by D-DNP, stored in the holding chamber for a time τ_{TSI}, and converted into LLS on malate by the enzyme. The remaining peaks of fumarate and HDO in the spectrum of Figure 5b probably stem from hyperpolarized single-quantum magnetization that was not fully saturated by the WALTZ-16 pulse train and was brought into the active volume of the *rf* coil by convection.

Conclusion

We have shown that a pure TSI can be created readily by D-DNP in a system that contains two magnetically equivalent spins in solution. Once dissolved, this imbalance displays a lifetime T_{TSI} that is much longer than the longitudinal relaxation time T_1. We believe this to be the first proof of principle of the creation of hyperpolarized long-lived states for equivalent spins (HELLS) by D-DNP. Such a long-lived spin order can be used readily to monitor a slow enzymatic process of biochemical relevance, but may find applications in other areas of magnetic resonance such as imaging (MRI), for which hyperpolarization by D-DNP has become a technique of choice to enable metabolic imaging, and in which short lifetimes of hyperpolarized molecules are usually a major limitation. The HELLS methodology will be applied to more challenging molecules containing magnetically equivalent pairs of spins, such as CH_2RR', CH_2Cl_2, and possibly H_2O. We are currently investigating molecules with interesting lifetimes and interesting chemical or biochemical properties that can be addressed by HELLS. As fumarate plays a crucial role in the Krebs cycle, it may be of interest for in vivo studies as it has been demonstrated to be a probe for cellular necrosis.[18]

Experimental Section

DNP samples

Solutions of 0.5 M dibasic sodium fumarate (Sigma–Aldrich) in the glass-forming mixture D_2O:[D_6]ethanol (60:40 v/v) were doped with 50 mM TEMPOL (Sigma–Aldrich). Ethanol was added drop by drop to avoid precipitation. The solution was then sonicated for 10 min. Ten frozen pellets of 10 μL each of this mixture were inserted in the polarizer, along with ten frozen pellets of 10 μL each containing 3 M ascorbate (Sigma–Aldrich) in D_2O to scavenge the radicals after dissolution.[17]

DNP polarization and dissolution

DNP was performed at 1.2 K and 6.7 T in a home-built polarizer by applying frequency-modulated microwave irradiation[19] at $f_{\mu W} = 188.3$ GHz and $P_{\mu W} = 100$ mW, with a modulation frequency of 10 kHz and modulation amplitude of 50 MHz. The polarized pellets were dissolved in 0.7 s with 5 mL D_2O, preheated to $T = 400$ K at $P = 1.0$ MPa, and transferred in 4.5 s to a 7 T (300 MHz) magnet by pushing with helium gas at 0.6 MPa through a PTFE tube (1.5 mm inner diameter) running through a magnetic tunnel (3 m length).

Enzymatic detection

The hyperpolarized solution was kept at $B_0 > 6.5$ T in a holding chamber just above the NMR sample tube for a variable delay τ_{TSI} to monitor the relaxation of the TSI of fumarate. The sample was then injected in 2 s into an NMR tube containing D_2O (200 μL) for field-frequency locking, NaCl (200 mM) and TRIS buffer (25 mM), and fumarase (5 μL, 5.8 mg mL^{-1}, 12.5 units) from porcine heart (Sigma–Aldrich). Finally, the LLS detection sequence described in Figure 3 was applied with n sustaining delays of $\tau_{LLS} = 6$ s each with WALTZ-16 irradiation.

Acknowledgements

We are indebted to Pascal Miéville, Martial Rey, and Anto Barisic for valuable assistance. This work was supported by the Swiss National Science Foundation (SNSF), the Swiss Commission for Technology and Innovation (CTI), the EPFL, the French CNRS, and the ERC (advanced grant "dilute *para*-water").

Keywords: dynamic nuclear polarization · enzymes · long-lived states · NMR spectroscopy · triplet–singlet imbalance

[1] a) J. H. Ardenkjaer-Larsen, B. Fridlund, A. Gram, G. Hansson, L. Hansson, M. H. Lerche, R. Servin, M. Thaning, K. Golman, *Proc. Natl. Acad. Sci. USA* **2003**, *100*, 10158 – 10163.

[2] a) S. E. Day, M. I. Kettunen, F. A. Gallagher, D. E. Hu, M. Lerche, J. Wolber, K. Golman, J. H. Ardenkjaer-Larsen, K. M. Brindle, *J. Nat. Med.* **2007**, *13*, 1382 – 1387; b) M. Karlsson, P. R. Jensen, J. O. Duus, S. Meier, M. H. Lerche, *Appl. Magn. Reson.* **2012**, *43*, 223 – 236.

[3] a) R. Buratto, A. Bornet, J. Milani, D. Mammoli, B. Vuichoud, N. Salvi, M. Singh, A. Laguerre, S. Passemard, S. Gerber-Lemaire, S. Jannin, G. Bodenhausen, *ChemMedChem.* **2014**. DOI: 10.1002/cmdc.201402214; b) T. Harris, O. Szekely, L. Frydman, *J. Phys. Chem. B* **2014**, *118*, 3281 – 3290; c) Y. Lee, H. F. Zeng, A. Mazur, M. Wegstroth, T. Carlomagno, M. Reese, D. Lee, S. Becker, C. Griesinger, C. Hilty, *Angew. Chem.* **2012**, *124*, 5269 – 5272; *Angew. Chem. Int. Ed.* **2012**, *51*, 5179 – 5182.

[4] A. Bornet, R. Melzi, A. J. Perez-Linde, P. Hautle, B. van den Brandt, S. Jannin, G. Bodenhausen, *J. Phys. Chem. Lett.* **2013**, *4*, 111 – 114.

[5] M. H. Levitt, *Annu. Rev. Phys. Chem.* **2012**, *63*, 89 – 105.

[6] a) P. R. Vasos, A. Comment, R. Sarkar, P. Ahuja, S. Jannin, J. P. Ansermet, J. A. Konter, P. Hautle, B. van den Brandt, G. Bodenhausen, *Proc. Natl. Acad. Sci. USA* **2009**, *106*, 18469 – 18473; b) W. S. Warren, E. Jenista, R. T. Branca, X. Chen, *Science* **2009**, *323*, 1711 – 1714; c) P. Ahuja, R. Sarkar, S. Jannin, P. R. Vasos, G. Bodenhausen, *Chem. Commun.* **2010**, *46*, 8192 – 8194; d) A. Bornet, S. Jannin, G. Bodenhausen, *Chem. Phys. Lett.* **2011**, *512*, 151 – 154; e) C. Laustsen, G. Pileio, M. C. D. Tayler, L. J. Brown, R. C. D. Brown, M. H. Levitt, J. H. Ardenkjaer-Larsen, *Magn. Reson. Med.* **2012**, *68*, 1262 – 1265; f) M. C. D. Tayler, I. Marco-Rius, M. I. Kettunen, K. M. Brindle, M. H. Levitt, G. Pileio, *J. Am. Chem. Soc.* **2012**, *134*, 7668 – 7671; g) I. Marco-Rius, M. C. D. Tayler, M. I. Kettunen, T. J. Larkin, K. N. Timm, E. M. Serrao, T. B. Rodrigues, G. Pileio, J. H. Ardenkjaer-Larsen, M. H. Levitt, K. M. Brindle, *NMR Biomed.* **2013**, *26*, 1696 – 1704; h) G. Pileio, S. Bowen, C. Laustsen, M. C. D. Tayler, J. T. Hill-Cousins, L. J. Brown, R. C. D. Brown, J. H. Ardenkjaer-Larsen, M. H. Levitt, *J. Am. Chem. Soc.* **2013**, *135*, 5084 – 5088.

[7] a) G. Pileio, *Prog. Nucl. Magn. Reson. Spectrosc.* **2010**, *56*, 217 – 231; b) M. Carravetta, M. H. Levitt, *J. Chem. Phys.* **2005**, *122*, 214505; c) G. Pileio, M. H. Levitt, *J. Chem. Phys.* **2009**, *130*, 214501.

[8] B. Meier, J. N. Dumez, G. Stevanato, J. T. Hill-Cousins, S. S. Roy, P. Hakansson, S. Mamone, R. C. D. Brown, G. Pileio, M. H. Levitt, *J. Am. Chem. Soc.* **2013**, *135*, 18746 – 18749.

[9] a) C. R. Bowers, D. P. Weitekamp, *J. Am. Chem. Soc.* **1987**, *109*, 5541 – 5542; b) T. C. Eisenschmid, R. U. Kirss, P. P. Deutsch, S. I. Hommeltoft, R. Eisenberg, J. Bargon, R. G. Lawler, A. L. Balch, *J. Am. Chem. Soc.* **1987**, *109*, 8089 – 8091; c) S. Glöggler, J. Colell, S. Appelt, *J. Magn. Reson.* **2013**, *235*, 130 – 142.

[10] V. V. Zhivonitko, K. V. Kovtunov, P. L. Chapovsky, I. V. Koptyug, *Angew. Chem.* **2013**, *125*, 13493 – 13497; *Angew. Chem. Int. Ed.* **2013**, *52*, 13251 – 13255.

[11] Y. N. Zhang, P. C. Soon, A. Jerschow, J. W. Canary, *Angew. Chem.* **2014**, *126*, 3464 – 3467; *Angew. Chem. Int. Ed.* **2014**, *53*, 3396 – 3399.

[12] M. Carravetta, M. H. Levitt, *J. Am. Chem. Soc.* **2004**, *126*, 6228 – 6229.

[13] M. Carravetta, O. G. Johannessen, M. H. Levitt, *Phys. Rev. Lett.* **2004**, *92*, 153003.

[14] M. C. D. Tayler, M. H. Levitt, *Phys. Chem. Chem. Phys.* **2011**, *13*, 5556 – 5560.

[15] a) K. Nagashima, S. S. Velan, *Concepts Magn. Reson. Part A* **2013**, *42*, 165 – 181; b) R. Sarkar, P. R. Vasos, G. Bodenhausen, *J. Am. Chem. Soc.* **2007**, *129*, 328 – 334.

[16] R. Sarkar, P. Ahuia, D. Moskau, P. R. Vasos, G. Bodenhausen, *ChemPhysChem* **2007**, *8*, 2652 – 2656.

[17] a) P. Miéville, P. Ahuja, R. Sarkar, S. Jannin, P. R. Vasos, S. Gerber-Lemaire, M. Mishkovsky, A. Comment, R. Gruetter, O. Ouari, P. Tordo, G. Bodenhausen, *Angew. Chem.* **2010**, *122*, 6318 – 6321; *Angew. Chem. Int. Ed.* **2010**, *49*, 6182 – 6185; b) Corrigendum: P. Miéville, P. Ahuja, R. Sarkar, S. Jannin, P. R. Vasos, S. Gerber-Lemaire, M. Mishkovsky, A. Comment, R. Gruetter, O. Ouari, P. Tordo, G. Bodenhausen, *Angew. Chem.* **2010**, *122*, 8004 – 8004; *Angew. Chem. Int. Ed.* **2010**, *49*, 7834 – 7834.

[18] F. A. Gallagher, M. I. Kettunen, D. E. Hu, P. R. Jensen, R. in't Zandt, M. Karlsson, A. Gisselsson, S. K. Nelson, T. H. Witney, S. E. Bohndiek, G. Hansson, T. Peitersen, M. H. Lerche, K.M. Brindle, *Proc. Natl. Acad. Sci. USA* **2009**, *106*, 19801 – 19806.

[19] A. Bornet, J. Milani, B. Vuichoud, A. J. Perez-Linde, G. Bodenhausen, S. Jannin, *Chem. Phys. Lett.* **2014**, *602*, 63 – 67.

Received: August 22, 2014
Published online on October 24, 2014

